Biophysical Journal, Volume *112*

Supplemental Information

SNARE-Mediated Single-Vesicle Fusion Events with Supported and Freestanding Lipid Membranes

Jan W. Kuhlmann, Meike Junius, Ulf Diederichsen, and Claudia Steinem

Supporting Information

SNARE-mediated single vesicle fusion events with supported and freestanding lipid membranes

Jan W. Kuhlmann, Meike Junius, Ulf Diederichsen, and Claudia Steinem*

Institute of Organic and Biomolecular Chemistry, University of Göttingen, Tammannstr. 2, 37077 Göttingen, Germany

1. Docking time distribution

Docking times of the syb 2 containing vesicles were extracted from individual time series. Due to the finite time window of 155 s of each time series the number of events is generally underestimated with larger docking times. If the number of docking events was constant throughout the entire time series, a correction would be necessary to account for the longer docking times. However, in our experiments we inject the syb 2 containing vesicles at the beginning of each time series resulting in an initially high local concentration of vesicles that dilutes over time. Accordingly, the majority of vesicles (70%) dock within the first 50 s of the time series of 155 s (Fig. S1). As 80% of the entire docking times are distributed within the first 50 s of the time series, it can safely be assumed that the docking times are not significantly influenced by the finite observation window in the region of 0-80 s making a correction unnecessary.

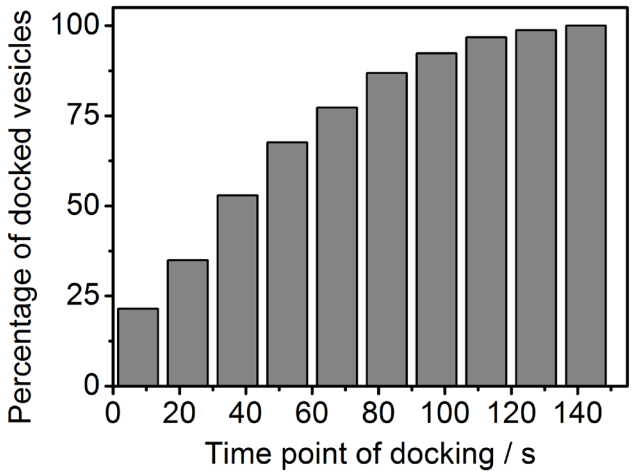

Figure S1. Cumulative distribution function of syb 2 containing vesicles (n = 312) showing the time point of docking within the 155 s long time series. Due to the manual injection of the vesicles at the beginning of each time series, most of the vesicles (~70%) dock within the first 50 s of the time window.

2. Vesicle size

Syb 2 containing vesicles were prepared by extrusion through a polycarbonate membrane with a nominal pore size of 400 nm (Avestin, Ottawa, USA). We determined the size of the vesicles by dynamic light scattering (DLS) in reconstitution buffer (Fig. S2). The vesicles have an average diameter of 240 ± 100 nm.

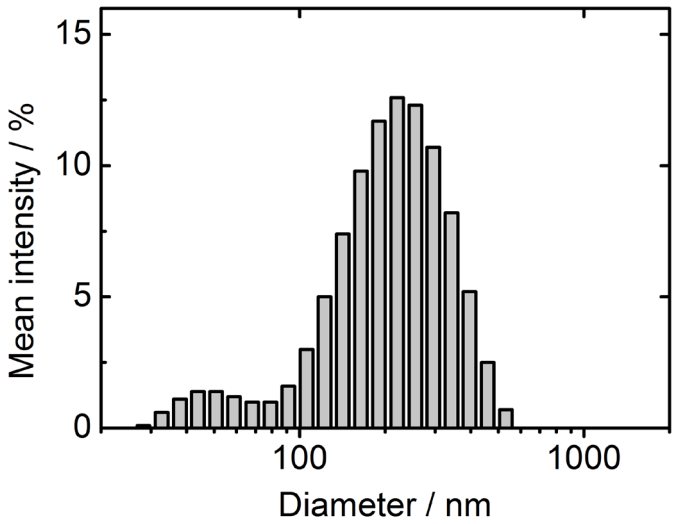

Figure S2. Size distribution of syb 2 doped vesicles extruded through polycarbonate membranes with a nominal pore diameter of 400 nm measured by means of dynamic light scattering.

3. Mobility of SNAREs in s-PSMs

We determined the diffusion constants of the fluorescently labeled lipid Atto488-DPPE and the fluorescently labeled OregonGreen-syntaxin 1A-transmembrane domain (OG-syx 1A TMD) on the s-PSM by indirect FRAP experiments. Due to the gold-induced fluorescence quenching, it is not possible to measure the mobility on the s-PSM directly. Therefore, indirect FRAP experiments were performed by bleaching an entire f-PSM labeled either with 1 mol% Atto488-DPPE or OG-syx 1A TMD and measuring the fluorescence recovery in the f-PSM (Fig. S3A). As the f-PSM is completely surrounded by s-PSM, any observed fluorescence recovery into the f-PSM results from a mobile fraction of molecules in the s-PSM. If the molecules were fully immobile in the s-PSMs, no recovery into the bleached f-PSM would be monitored. Normalized fluorescence recovery curves obtained after indirect FRAP on f-PSMs that were doped either with Atto488-DPPE or OG-syx 1A TMD are shown in Fig. S3B. An apparent diffusion constant for Atto488-DPPE was determined from the recovery curve with $D_{DPPE} = 2.8 \pm 0.4$ μm^2/s (SD), $n = 9$. For OG-syx 1A TMD the diffusion constant was determined to be $D_{syx1A} = 1.1 \pm 0.2$ μm^2/s (SD), $n = 6$. The diffusion coefficients are similar to those obtained on solid supported SiO_2 and polymer-cushioned membranes (1, 2). The 2-3 times lower diffusion coefficient of OG-syx 1A TMD compared to the lipid Atto488-DPPE is due to the fact that the TMD is anchored in both leaflets of the lipid bilayer and has a larger cross sectional area than a single lipid. The reduced diffusion constant of OG-syx 1A TMD compared to Atto488-DPPE was also found in f-PSMs (3). It is important to note that the applied indirect FRAP experiments always yield a 100% fluorescence recovery, as the components in the f-PSM are 100% mobile and only the mobile fraction of proteins and lipids of the s-PSMs diffuse into the f-PSM and are detected. A mobile fraction in the s-PSM cannot be determined from these experiments.

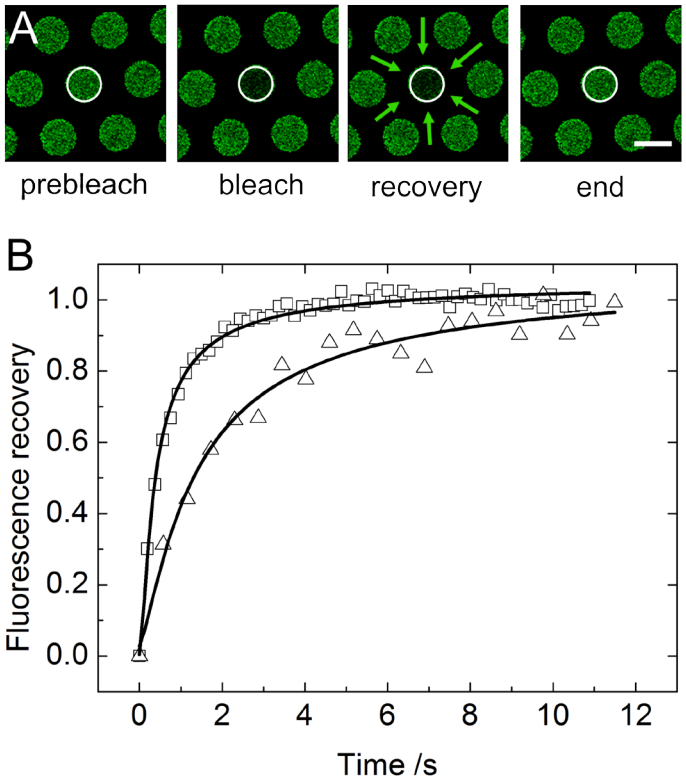

Figure S3. Lateral diffusion of Atto488-DPPE and OG-syx 1A TMD composed of DOPC/POPS/POPE/cholesterol (5:1:2:2). (**A**) Fluorescence micrograph snapshots obtained from an indirect FRAP experiment performed on PSMs doped with 0.8 mol% OG-syx 1A TMD showing the bleached area (white circle = ROI) with a radius of 2.2 µm. Scale bar: 5 µm. (**B**) Time dependent fluorescence recovery of Atto488-DPPE (squares) and OG-syx 1A TMD (rectangles) analyzed in the ROI with radius of 2.2 µm. Diffusion coefficients were derived from mono exponential fits (solid lines) yielding 2.8 $\mu m^2/s$ for Atto488-DPPE and 1.1 $\mu m^2/s$ for OG-syx 1A TMD.

4. Observation of lipid mixing

Lipid mixing of vesicles that fuse with PSMs could be experimentally visualized by analyzing the Texas Red-DPPE (TR) intensity in a 4×4 $pixel^2$ region of interest (ROI) on the center of the vesicle and in a donut-shaped ROI with a thickness of 2 pixels around the vesicle (Fig. S4A).

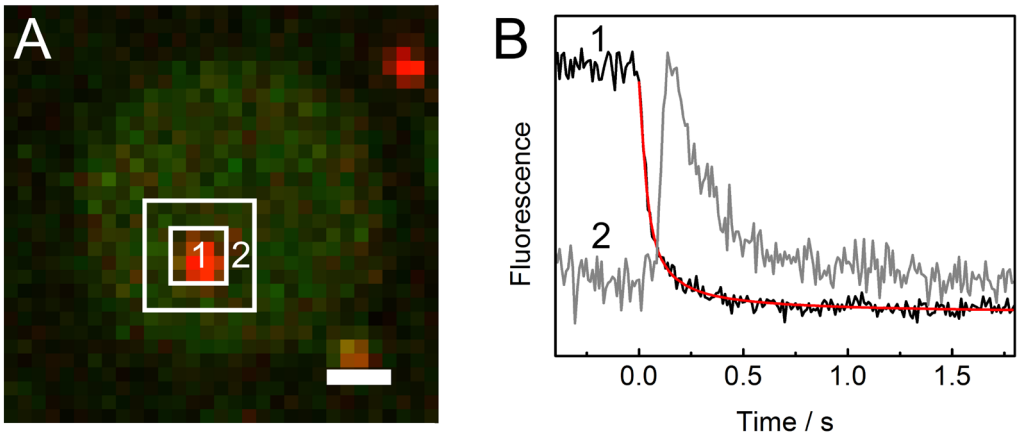

Figure S4. (**A**) Fluorescence micrograph depicting a syb 2 doped vesicle docked to a ΔN49-complex containing f-PSM prior to fusion. The center ROI (1) and the donut-shaped ROI (2) are used to read out the TR fluorescence intensities at the onset of fusion. Scale bar: 1 µm. (**B**) Corresponding intensity vs. time trace of ROI (1) and (2) obtained during fusion of the vesicle with the f-PSM. The TR decay in the center ROI was modeled assuming a disc source of lipids with radius 0.5 µm that diffuses in the surrounding membrane with a diffusion coefficient of 2 $\mu m^2/s$ (red curve).

Upon onset of fusion, the TR diffuses radially away from the vesicle ghost resulting in the observable TR decay. At the same time, TR diffuses into the surrounding donut shaped ROI resulting in an increase in TR fluorescence intensity which then slowly decreases when the fluorophore dilutes in the PSM (Fig. S4B). The TR decay observed in the center ROI (1) can be modeled by assuming a lipid disc source with a radius of 0.5 µm that diffuses into the surrounding membrane with a diffusion coefficient of 2 $\mu m^2/s$ (red curve in Fig. S4B). This confirms that lipid mixing between the vesicle and the PSM occurs, which can be reliably identified by the TR decay.

5. Intermediate TR-DPPE release

We observed that 13% of the s-PSM fusion events showed a TR intensity that dropped to an intermediate fluorescence level between that observed for the docked state and that before the onset of docking (Fig. S5A). All events show a relative TR intensity level of 50% and below (Fig. S5B). Moreover, all observed events with intermediate TR intensities show an Atto488 dequenching signal if dual color mode fluorescence experiments were performed (data not shown) indicating that the Atto488 fluorophore is lifted off from the support.

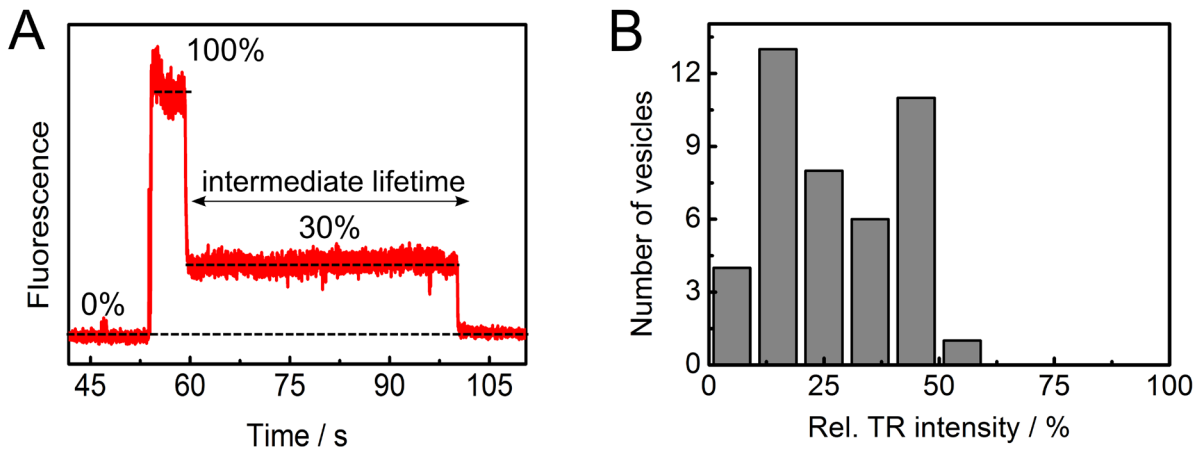

Figure S5. (**A**) Characteristic time resolved TR intensity trace of a fusion event with a relative TR level above the intensity prior to the onset of docking (30%). The TR intensity decreases to the baseline level in a second step after a certain time period, which is called intermediate lifetime. (**B**) Histogram analysis of the relative TR intensities of those events that show an intermediate level (n = 42, 13%).

Such intermediate levels could arise from fusion intermediates like hemifusion (4-10). In case of hemifusion, a distribution around 50% would be expected as only the outer membrane leaflet fused with the target membrane. However, a larger number of events show a relative TR intensity below 50% indicating that a hemifusion intermediate cannot fully explain this observation. Transient fusion pores that randomly reseal, resulting in the partial merging of the vesicle membrane with the PSM or a smaller vesicle enclosed in the larger fusing vesicle (11) that is released under the membrane, could alternatively explain the observed intensity levels well below 50%.

6. Videos of diffusing and fusing vesicles

Movie S1 (still image in Fig. S6A) shows the observed time series of a docked vesicle that fuses with the f-PSM and Movie S2 (still image in Fig. S6B) shows a vesicle that fuses with the s-PSM. Both videos were recorded with 96 frames per seconds.

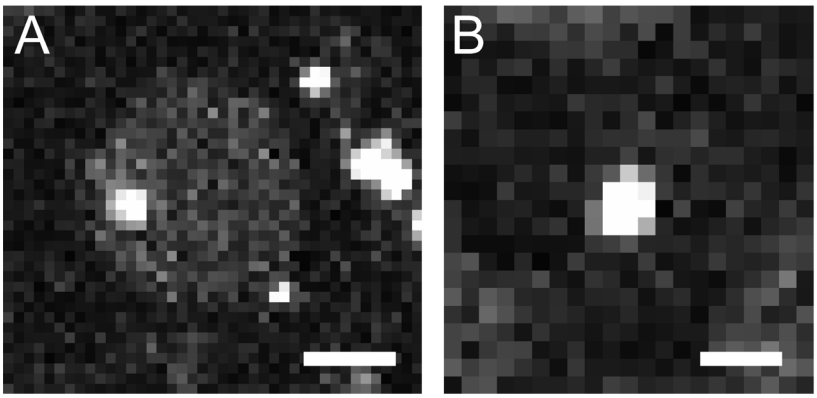

Figure S6. Snapshots of (**A**) Movie S1 and (**B**) Movie S2 showing a syb 2-containing vesicle composed of DOPC/POPS/POPE/cholesterol (5:1:2:2) doped with TR docked to a ΔN49-complex-containing (**A**) f-PSM and (**B**)s-PSM, respectively. The PSM is composed of DOPC/POPS/POPE/cholesterol (5:1:2:2) and doped with Atto488-DPPE. Both videos are shown with a two times reduced frame rate. Scale bars: 2 μm.

Supporting References

1. Wagner, M. L., and L. K. Tamm, 2001. Reconstituted syntaxin1A/SNAP25 interacts with negatively charged lipids as measured by lateral diffusion in planar supported bilayers. *Biophys. J.* 81:266–275.

2. Bowen, M. E., K. Weninger, A. T. Brunger, and S. Chu, 2004. Single molecule observation of liposome-bilayer fusion thermally induced by soluble N-ethyl maleimide sensitive-factor attachment protein receptors (SNAREs). *Biophys. J.* 87:3569–3584.

3. Schwenen, L. L. G., R. Hubrich, D. Milovanovic, B. Geil, J. Yang, A. Kros, R. Jahn, and C. Steinem, 2015. Resolving single membrane fusion events on planar pore-spanning membranes. *Sci. Rep.* 5:1–15.

4. Kreutzberger, A. J., V. Kiessling, and L. K. Tamm, 2015. High cholesterol obviates a prolonged hemifusion intermediate in fast SNARE-mediated membrane fusion. *Biophys. J.* 109:319–329.

5. Yoon, T.-Y., B. Okumus, F. Zhang, Y.-K. Shin, and T. Ha, 2006. Multiple intermediates in SNARE-induced membrane fusion. *Proc. Natl. Acad. Sci. U.S.A.* 103:19731–19736.

6. Hernandez, J. M., A. Stein, E. Behrmann, D. Riedel, A. Cypionka, Z. Farsi, P. J. Walla, S. Raunser, and R. Jahn, 2012. Membrane fusion intermediates via directional and full assembly of the SNARE complex. *Science* 336:1581–1584.

7. Lu, X., 2005. Membrane fusion induced by neuronal SNAREs transits through hemifusion. *J. Biol. Chem.* 280:30538–30541.

8. Liu, T., T. Wang, E. R. Chapman, and J. C. Weisshaar, 2008. Productive hemifusion intermediates in fast vesicle fusion driven by neuronal SNAREs. *Biophys. J.* 94:1303–1314.

9. Giraudo, C. G., C. Hu, D. You, A. M. Slovic, E. V. Mosharov, D. Sulzer, T. J. Melia, and J. E. Rothman, 2005. SNAREs can promote complete fusion and hemifusion as alternative outcomes. *J. Cell Biol.* 170:249–260.

10. Elhamdani, A., 2006. Double patch clamp reveals that transient fusion (kiss-and-run) is a major mechanism of secretion in calf adrenal chromaffin cells: high calcium shifts the mechanism from kiss-and-run to complete fusion. *J. Neurosci.* 26:3030–3036.

11. Parmar, M. M., K. Edwards, and T. D. Madden, 1999. Incorporation of bacterial membrane proteins into liposomes: factors influencing protein reconstitution. *Biochim. Biophys. Acta, Biomembr.* 1421:77–90.